

Temperature-Dependent Optical Kerr Effect Spectroscopy of Aromatic Liquids

Brian J. Loughnane,[†] Alessandra Scodinu,[†] and John T. Fourkas^{*,‡}

Eugene F. Merkert Chemistry Center, Boston College, Chestnut Hill, Massachusetts 02467, and Department of Chemistry and Biochemistry, University of Maryland, College Park, Maryland 20742

Received: October 3, 2005; In Final Form: January 23, 2006

Ultrafast optical Kerr effect (OKE) spectroscopy has been used to study the temperature-dependent dynamics of five aromatic liquids: benzene, benzene-*d*₆, hexafluorobenzene, mesitylene, and 1,3,5-trifluorobenzene. The intermediate response time of all of the liquids was found to scale with the collective orientational correlation time, as has been observed for other simple liquids. The spectra of hexafluorobenzene, 1,3,5-trifluorobenzene, and mesitylene are qualitatively different from those of the other liquids and exhibit different behavior with temperature. These spectra allow us to assess the influence of different molecular parameters on the shape of the OKE spectrum. On the basis of these data, we propose a model that links the differences in the OKE spectra to corresponding differences in the local ordering of the liquids.

I. Introduction

The microscopic motions of liquids play a key role in chemical processes in solution, and as a result, a considerable amount of effort has been spent studying intermolecular liquid dynamics in recent years. One popular technique for studying the microscopic dynamics of liquids is optical Kerr effect (OKE) spectroscopy.^{1–4} In a typical OKE experiment, a vertically polarized pump laser pulse is incident on a transparent liquid sample, inducing a transient birefringence via a Raman process. The decay of this birefringence is probed through the time dependence of the degree of ellipticity induced in a second, probe laser pulse that is polarized at 45° with respect to the pump pulse. The OKE decay yields information on the diffusive reorientation of the molecules as well as on the low-frequency, Raman-active modes of the liquid. As an additional means of gaining insight into the low-frequency modes of the liquid, Fourier transform deconvolution techniques pioneered by McMorro and Lotshaw^{5–7} can be used to convert time-domain OKE data into a Bose–Einstein-corrected, low-frequency, depolarized Raman spectrum.

Despite the fact that OKE spectroscopy is a well-established technique, considerable challenges remain in extracting as much information as possible from OKE data. For instance, it is well understood that the long-time decay in the OKE signal arises from orientational diffusion. In liquids composed of molecules with sufficiently high symmetry, this tail generally takes the form of a single exponential.⁸ However, if this exponential is subtracted from the data, a second, faster exponential is usually evident.^{7,9–20} The origin of this “intermediate response” remains a matter of debate. We have shown previously, for a series of liquids composed of linear or symmetric-top molecules, that the intermediate response time tracks the orientational diffusion time as the temperature is varied.^{16,20} This observation, which has subsequently been verified for other, less symmetric liquids,¹⁸ suggests that the intermediate response has a hydrodynamic origin. On this basis, we proposed that the intermo-

lecular response is related to motional narrowing of intermolecular modes.¹⁶ Although this idea has received support from subsequent studies by other groups,^{19,21} the source of the intermolecular response remains very much an open question.

In analyzing OKE data in the frequency domain, it is common to remove the component of the signal due to diffusive reorientation, leaving what is often called the reduced spectral density (RSD).⁷ Developing a microscopic interpretation of the RSD is another major challenge in OKE spectroscopy. In simple molecular liquids, the RSD shows relatively little structure. The RSD can often be described as being composed of two superimposed features. It has been shown for liquids such as CS₂,¹⁶ acetonitrile,¹⁶ and benzene,^{1,19} that, as the temperature of a liquid is lowered, the high-frequency feature moves to higher frequencies and the low-frequency feature moves to lower frequencies. The behavior of the high-frequency feature is often explained in terms of a stiffening of the intermolecular potential as the density of the liquid increases with lowering temperature. The behavior of the low-frequency feature is more difficult to explain but, again, is consistent with motional narrowing.

In many liquids, the RSD can be fit well to the sum of two contributions, a Bucaro–Litovitz (BL) function and an antisymmetrized Gaussian (AG).^{13,14,18,22–24} The former function was developed to describe depolarized light scattering in noble-gas fluids.²⁵ In these systems, scattering necessarily arises from many-body effects that involve only translational motions. As a result, the BL portion of the fit in OKE RSDs is often attributed to hindered translational motions, whereas the AG component is credited to hindered rotational motions. Although it is generally true that hindered translational motions have lower frequencies than do hindered rotational motions, it has become clear that this interpretation of the fits to the RSD is considerably oversimplified. Indeed, there is currently no theoretical basis for expecting that RSDs should be described by the sum of a BL function and an AG function. Although it is tempting to assign microscopic significance to the six parameters used in such fits, one extreme viewpoint is that this number of parameters is sufficient to describe a wide variety of spectral shapes without having any underlying meaning. This is another issue that requires further investigation.

* To whom correspondence should be addressed. E-mail: fourkas@umd.edu.

[†] Boston College.

[‡] University of Maryland.

TABLE 1: Molecular Weights, Moments of Inertia, Isotropic Polarizabilities, Polarizability Anisotropies, and Quadrupole Moments of the Liquids Studied Here

liquid	MW (amu)	I_x (10^{-45} kg-m ²)	α_{iso} (\AA^3)	$\Delta\alpha$ (\AA^3)	Q (10^{-40} C m ²)
benzene	78.11	1.43 ⁸¹	11.56 ¹⁴	-5.19 ¹⁴	-30.0 ¹⁴
benzene- <i>d</i> ₆	84.15	1.75 ⁸²	11.56 ^a	-5.19 ^a	-30.0 ^a
mesitylene	120.19	4.29 ⁸¹	16.18 ⁸³	-7.97 ⁸³	-32.6 ⁸⁴
TFB	132.08	4.75 ¹⁴	11.3 ¹⁴	-7.20 ¹⁴	3.1 ¹⁴
HFB	186.05	8.21 ¹⁴	11.65 ¹⁴	-7.50 ¹⁴	31.7 ¹⁴

^a The actual values of the isotropic polarizability, the polarizability anisotropy, and the quadrupole moment of benzene-*d*₆ are probably a few percent less than those of benzene, but no measured values could be found in the literature.

Ryu and Stratt recently performed an illuminating study in which molecular dynamics (MD) simulations and an instantaneous normal mode (INM) analysis of benzene made it possible to begin to dissect the RSD for this liquid on a molecular level.²⁶ This is an attractive system, as benzene and its derivatives have been the subjects of a large number of experimental OKE studies.^{1,14,16,18,19,21,24,26-42} At room temperature, the RSDs for these liquids differ from those of liquids composed of linear molecules (although in both cases the fitting function described above generally does a good job of describing the OKE data). The RSDs for benzene and its derivatives tend to be broad with a relatively flat top at room temperature, whereas the reduced spectral densities for linear molecules such as CS₂ and acetonitrile are more rounded. These differences have led some researchers to suggest that there is a special low-frequency band in the benzene RSD that arises from long-lived dimers.³¹ However, subsequent studies of CS₂ and acetonitrile at low temperature¹⁵ revealed RSDs that closely resemble that of benzene at room temperature, suggesting that a single basic model can probably describe the OKE spectra of all of these liquids.

Ryu and Stratt suggested that the shapes of the RSDs of benzene and its derivatives are largely a function of molecular shape.²⁶ In particular, they pointed out that, because benzene and its derivatives have two relatively low moments of inertia, their hindered reorientational motions span a larger frequency range than do their hindered translational motions. In contrast, the molecules in a liquid such as CS₂ have a single relatively large moment of inertia, and therefore, there is not such a large frequency separation between hindered rotations and translations.

With all of these ideas in mind, we present here detailed temperature-dependent OKE studies of five aromatic liquids: benzene, benzene-*d*₆, 1,3,5-trifluorobenzene (TFB), hexafluorobenzene (HFB), and mesitylene (1,3,5-trimethylbenzene). The temperature-dependent OKE spectroscopy of benzene has been studied previously by us^{1,16} and by others,¹⁹ but is an important reference point for the study of the other liquids. HFB and TFB have been studied only at room temperature,¹⁴ and benzene-*d*₆ and mesitylene have not been studied at all with OKE spectroscopy to our knowledge. All of these liquids are sufficiently symmetric that they should exhibit single-exponential orientational diffusion,⁸ allowing their reduced spectral densities to be determined with great precision. Although the molecules all have similar shapes, other important physical parameters change considerably from molecule to molecule, as shown in Table 1. Furthermore, detailed neutron scattering and molecular dynamics data are available for benzene,^{26,34,43-47} TFB,⁴⁸⁻⁵⁰ and HFB.^{43,44,46,47,51} Taken together, these liquids provide a means for gaining a deeper understanding of the microscopic origin of the OKE response.

II. Experimental Section

Viscosity measurements were made with an Ubbelohde viscometer, as described previously.¹⁶ Raman data were used to determine the single-molecule orientational correlation times, $\tau_{\text{or,sm}}$, for benzene,⁵² HFB,⁵³ mesitylene,⁵³ and TFB.⁵³ The Raman data were analyzed with the Debye–Stokes–Einstein (DSE) relation^{54,55}

$$\tau_{\text{or,sm}} \approx \frac{\eta V_{\text{H}}}{k_{\text{B}} T} \quad (1)$$

where η is the viscosity, V_{H} is the hydrodynamic volume for reorientation, k_{B} is Boltzmann's constant, and T is the temperature. A linear least-squares fit was made to a plot of $\tau_{\text{or,sm}}$ versus η/T for each liquid, and these fits were used to determine the single-molecule orientational correlation times at the temperatures used in the present study.

Our heterodyne-detected OKE experimental procedure has been described in detail elsewhere.^{15,56} All liquids were distilled and filtered before use, after which they were sealed in cuvettes with a 1-mm path length. To maintain temperature control, the cuvette was mounted to the coldfinger of a nitrogen-flow vacuum cryostat. A temperature sensor was mounted directly to the face of the cuvette near the point at which data were collected. The temperature was allowed to stabilize for 30 min after reaching the set point, and data collection was halted if the deviation from the set point was greater than 0.5 °C.

Averaged scans obtained at positive and negative heterodyne angles were subtracted from one another to obtain the pure heterodyne contribution to the OKE signal. The OKE signal is the negative time derivative of the collective orientational correlation function, $C_{\text{coll}}(\tau)$,⁵⁷ where τ is the delay time between the pump and probe pulses. Accordingly, $C_{\text{coll}}(\tau)$ can be computed by appropriate integration of the OKE decays.^{20,58,59} However, this procedure introduces an additional parameter, the constant of integration. If the decays have a clear functional form at long time, such as an exponential tail, this constant of integration can be determined with high accuracy. Furthermore, because integration removes high-frequency noise from the decay, the remaining parameters can be determined more accurately than is the case for unintegrated decays. A nonlinear least-squares routine⁶⁰ was used to fit $C_{\text{coll}}(\tau)$ to a biexponential decay with an adjustable baseline (constant of integration) at delay times greater than about 2 ps; somewhat longer starting times were used for the fits at lower temperatures. The two time constants, τ_{or} and τ_{i} , correspond to the collective orientational correlation time and the intermolecular response time, respectively, and the corresponding amplitudes are denoted A_{or} and A_{i} .

Once $C_{\text{coll}}(\tau)$ had been used to determine the functional form of the long-time tail of the OKE decay, this information was used to add a tail to the unintegrated OKE decay to extend the time range of the data. The Fourier transform deconvolution procedure of McMorro and Lotshaw⁷ was then applied to compensate for the effects of the finite duration of the laser pulses used. Once this procedure had been employed to determine the deconvolved response function, a function of the form

$$r(\tau) = A \exp(-\tau/\tau_{\text{or}})[1 - \exp(-\tau/\tau_{\text{i}})] \quad (2)$$

where A is an amplitude and τ_{i} is the rise time of the orientational alignment, was then subtracted from the response function to remove the contribution of orientational diffusion.

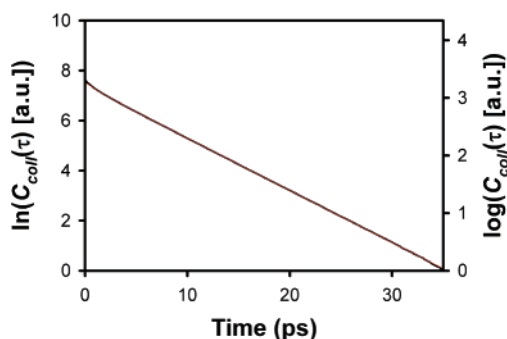


Figure 1. Integrated OKE decay for 1,3,5-trifluorobenzene at 335 K (black) and biexponential fit (red).

The rise time was chosen to be 200 fs, although the exact value did not affect the subsequent RSD significantly. The RSD was obtained by Fourier transformation of the response function from which the contribution of orientational diffusion had been removed. Where needed (vide infra), this procedure was repeated to remove the contribution of the intermediate response.

III. Results

Shown in Figure 1 is $C_{\text{coll}}(\tau)$ for TFB at 335 K, along with a biexponential fit to the data. The fit covers over seven factors of e and is in excellent agreement with the data. The quality of the integrated decay and fit is typical of the data for all five liquids at all of the temperatures studied. Tables of the parameters for the biexponential fits are provided in the Supporting Information. The amplitudes of the exponentials have been normalized such that $A_{\text{or}} + A_{\text{i}} = 1$. These data are also summarized in Figures 2–4.

The orientational correlation time in simple liquids generally follows the DSE relation^{54,55} (eq 1). A factor to account for the boundary conditions for reorientation is often incorporated in this equation as well. However, OKE spectroscopy measures a collective orientational correlation time, $\tau_{\text{or, coll}}$, which is given by the equation⁵⁵

$$\tau_{\text{or, coll}} = \frac{g_2}{j_2} \tau_{\text{or, sm}} \quad (3)$$

where g_2 is the static pair orientational correlation parameter and j_2 is the dynamic pair orientational correlation parameter. The latter parameter is generally assumed to take on a value near unity in simple liquids. The former parameter is a measure of the degree of parallel ordering in a liquid. Generally, g_2/j_2 depends only weakly on temperature, and so $\tau_{\text{or, coll}}$ also follows DSE-like behavior.

As shown in Figure 2a, the orientational correlation times for all of these liquids indeed follow DSE behavior; the slope of each plot is given in Table 2. The data for benzene and benzene- d_6 fall on the same line, as would be expected. The data for hexafluorobenzene and mesitylene fall roughly on one line as well. This suggests that the hydrodynamic volumes for reorientation are similar for these two liquids, which is reasonable given their structures. However, the slope for TFB is significantly higher than the slopes for HFB and mesitylene, despite the fact that TFB is somewhat smaller than either of these molecules.

Further comparison of the slopes of the DSE plots reveals additional mysteries. For molecules with the symmetries of those studied here, OKE spectroscopy is sensitive only to the tumbling reorientational motions. A molecular modeling program⁶¹ was used to estimate a plausible value of the hydrodynamic volume

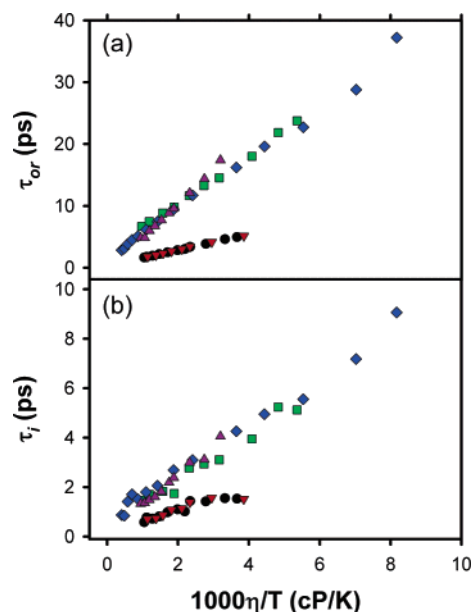


Figure 2. Temperature-dependent (a) slow and (b) fast time constants from biexponential fits to the integrated OKE decays for benzene (black), benzene- d_6 (red), HFB (green), mesitylene (blue), and TFB (purple).

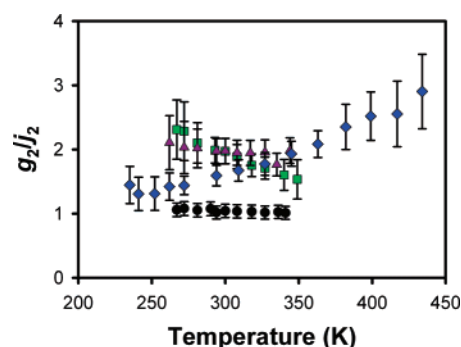


Figure 3. Values of g_2/j_2 calculated from OKE and Raman data for benzene (black), HFB (green), mesitylene (blue), and TFB (purple).

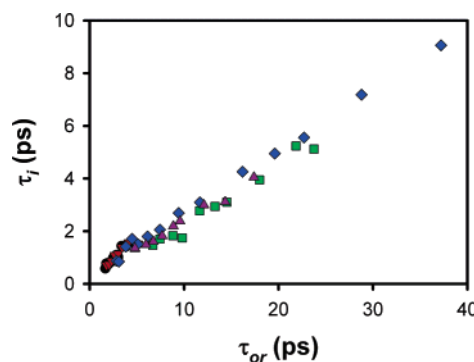


Figure 4. Fast versus slow time constants from biexponential fits at all temperatures for benzene (black), benzene- d_6 (red), HFB (green), mesitylene (blue), and TFB (purple).

for tumbling in each liquid, and these results are listed in Table 2. Also included in Table 2 are the ratios of the DSE slopes and hydrodynamic volumes of HFB, mesitylene, and TFB to those of benzene, as well as the ratio of the DSE slope ratio to the hydrodynamic volume ratio (which we denote ρ). In all cases, the ratio of DSE slopes is considerably greater than the ratio of hydrodynamic volumes. Although the calculated hydrodynamic volumes are only approximate, the error in these

TABLE 2: Comparison of DSE Slopes (m_{DSE}) and Hydrodynamic Volumes

liquid	m_{DSE} (ps K/cP)	V_{H} (\AA^3)	$m_{\text{DSE}}/m_{\text{DSE,ben}}$	$V_{\text{H}}/V_{\text{H,ben}}$	ρ
benzene	1270 ± 50	99			
benzene- d_6	1260 ± 50	99			
mesitylene	4120 ± 200	172	3.1	1.7	1.8
HFB	5630 ± 100	146	3.3	1.5	2.2
TFB	3890 ± 100	109	4.5	1.1	4.0

calculations cannot be great enough to account for the large differences in the two ratios for these three liquids.

If g_2/j_2 varies among these liquids, then it can also contribute to the value of ρ . To estimate the value of g_2 for these liquids as a function of temperature, we used our OKE data in conjunction with Raman data to compute g_2/j_2 . The results of these calculations are shown in Figure 3. For benzene, g_2/j_2 takes on a value near unity over the entire liquid temperature range. In HFB, g_2/j_2 has a value around 2.5 at low temperature and decreases to a value of approximately 1.5 near the boiling point, indicating an increase in the degree of perpendicular structure with increasing temperature. In TFB, g_2/j_2 takes on a value near 2 and is relatively insensitive to temperature. Finally, for mesitylene, g_2/j_2 is approximately 1.5 at low temperature and increases significantly with increasing temperature, indicating an increase in the degree of parallel ordering.

Because g_2/j_2 is approximately unity for benzene, in the absence of other effects, ρ should be approximately equal to g_2/j_2 for HFB, mesitylene, and TFB. The room-temperature value of g_2/j_2 for the HFB data in Figure 3 is approximately 2, which is close to the ρ value of 2.2. Similarly, the room-temperature value of g_2/j_2 for mesitylene is approximately 1.6, which is again also in good agreement with the value of ρ for this liquid. In the case of TFB, g_2/j_2 is also approximately 2 at room temperature, which is not in good agreement with the ρ value of 4.0 for this liquid.

As can be seen from Table 1, TFB has a quadrupole moment that is 1 order of magnitude smaller than those of the other liquids studied here. As a result, the microscopic structure of TFB is known to be considerably different from those of the other liquids.^{49,50} The large quadrupole moments of benzene, HFB, and mesitylene make face-to-face dimers high-energy structures, such that staggered parallel or perpendicular dimers are more energetically favorable. However, in the case of TFB, dispersion and octupole–octupole interactions can overcome the comparatively weaker quadrupole–quadrupole interactions to make face-to-face dimers energetically favorable. On the basis of neutron scattering experiments and MD simulations, such dimers are known to be prevalent in liquid TFB.^{49,50} These dimers contribute to the relatively large values of g_2 . In addition, if the dimers are long-lived, they can also lead to a significant increase in the hydrodynamic volume for tumbling. Alternatively, these dimers can be thought of as changing the boundary conditions from slip to partial stick. A combination of these effects should be sufficient to account for the observed value of ρ .

We have noted previously for a number of linear and symmetric-top liquids,^{16,20} including benzene,¹⁶ that the intermediate response time follows hydrodynamic behavior. As can be seen from Figure 2b, this is the case for all of the liquids studied here. There are also great similarities between the DSE plots for τ_{or} and τ_i , suggesting that the two times scale with one another. In Figure 4, we plot τ_i versus τ_{or} for all of these liquids. As was the case with the liquids that we studied previously,^{16,20} all of the data fall on a single straight line when

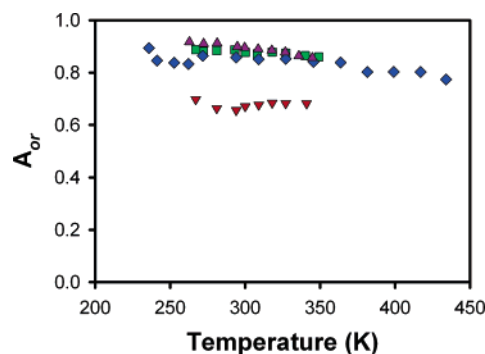


Figure 5. Relative amplitude of the slow exponential as a function of temperature in the biexponential fits for benzene (black), benzene- d_6 (red), HFB (green), mesitylene (blue), and TFB (purple).

plotted in this manner, which further supports our previous conjecture that there is a universal connection between these correlation times in simple liquids.¹⁶

In Figure 5, we plot the normalized amplitudes A_{or} corresponding to the portion of the orientational correlation function that is due to diffusive reorientation. For all of the liquids, this amplitude increases modestly as the temperature is lowered. The amplitudes for benzene and benzene- d_6 are essentially identical at all temperatures. The amplitudes for HFB, mesitylene, and TFB are all similar to one another and are considerably greater than those for the other two liquids. The significance of the normalized amplitude of the diffusive reorientation component is not clear at present, but Figure 5 reveals some intriguing trends. For instance, A_{or} correlates roughly with molecular size for these liquids. The microscopic implications of A_{or} are clearly a topic that merits further investigation.

We now turn to the reduced spectral densities. The RSDs for benzene, benzene- d_6 , and mesitylene over a broad range of temperatures are shown in Figure 6a–c, respectively. Temperature-dependent spectral densities are depicted for HFB in Figure 7a and for TFB in Figure 7b.

The temperature dependence of the RSD for benzene has been discussed in detail in other publications,^{1,19} but its qualitative features are worth brief consideration here as a basis for comparison to the RSDs of the other four liquids. At high temperature, the benzene RSD is smoothly curved, although it is skewed toward low frequency. As the temperature is decreased, the RSD flattens, and near the freezing point of benzene it appears distinctly bimodal. This behavior echoes that observed previously for CS_2 and acetonitrile,¹⁵ with a high-frequency feature that moves to higher frequency and a low-frequency feature that moves to lower frequency as the temperature is lowered. Indeed, as pointed out by Ryu and Stratt,²⁶ the shapes of the benzene RSDs are highly reminiscent of those for CS_2 and acetonitrile, although the temperature ranges in which the shapes change are somewhat different among the three liquids.

The RSDs of benzene- d_6 are similar to those of benzene at the corresponding temperatures, but are shifted to lower frequency, as would be expected from the higher mass and moment of inertia of benzene- d_6 . Insofar as the intermolecular response time scales with η/T and the viscosity of benzene- d_6 is greater than that of benzene at any given temperature, the RSD of benzene- d_6 at a particular temperature would not be expected to be an exact frequency-shifted version of the benzene RSD at the same temperature. Nevertheless, as shown in Figure 8, if the frequencies of the benzene- d_6 RSD at 300 K are multiplied by a factor of 1.1, there is a close correspondence with the RSD of benzene at this temperature. This same

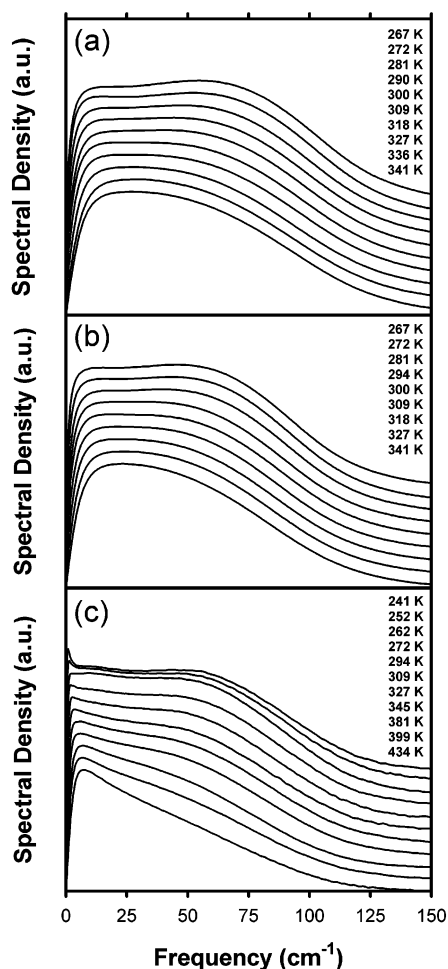


Figure 6. RSDs for (a) benzene, (b) benzene-*d*₆, and (c) mesitylene. The heights of the RSD have been normalized, and the offsets are for clarity.

correspondence holds across the entire liquid temperature range of these substances with the same factor of 1.1 in the frequency scaling. For hindered rotational modes of a single molecule, the frequency should scale with $(k/I_x)^{1/2}$, where k is the force constant for the mode and I_x is the moment of inertia for tumbling. For hindered translational modes of a single molecule, the frequency should scale with $(k/MW)^{1/2}$, where MW is the molecular weight. According to the data in Table 1, the scaling factor for hindered rotations should be 1.11, whereas that for hindered translations should be 1.04. It is difficult to tell the difference between these two scaling factors at the low frequencies at which translation might be expected to play a role in the RSD, but the excellent agreement between the benzene and benzene-*d*₆ RSDs when a scaling factor of 1.1 is used is at least suggestive of the idea that translational motions do not play a significant role in the benzene RSD. We shall revisit this issue below.

Although the RSDs for HFB and TFB are similar to one another, they are quite different from those for benzene. The RSDs for these two liquids take on an almost triangular appearance, with a prominent feature at low frequency that decays away relatively smoothly at high frequency. The RSDs for these liquids also exhibit far less of a temperature dependence than do those for benzene. With decreasing temperature, the low-frequency feature moves to lower frequencies, and there is some sign of the development of a hump at higher frequencies, particularly for HFB.

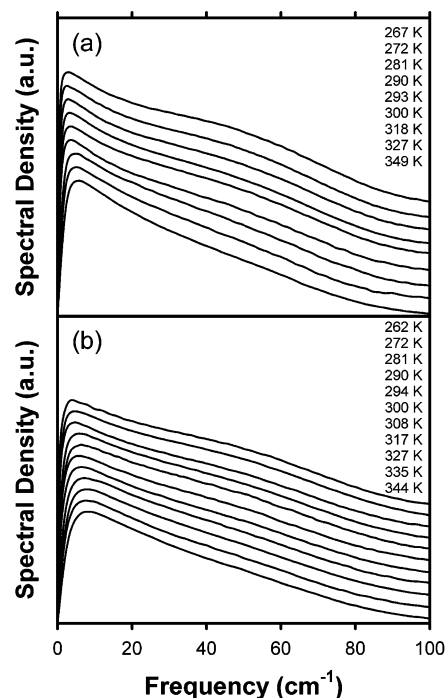


Figure 7. RSDs for (a) HFB and (b) TFB. The heights of the RSDs have been normalized, and the offsets are for clarity.

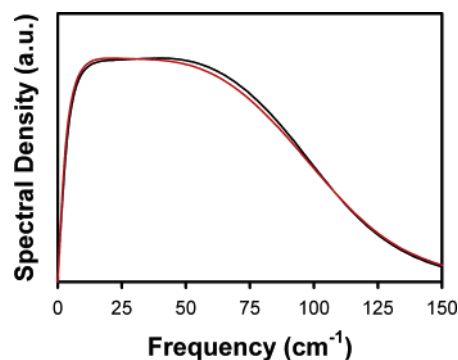


Figure 8. Comparison of the RSD for benzene at 300 K (black) with that of benzene-*d*₆ at the same temperature (red) with the frequencies scaled by a factor of 1.1.

One possible interpretation of the differences in the spectra of benzene and benzene-*d*₆ as compared to those of HFB and TFB is that the spectra of the latter two liquids are also effectively bimodal, but that the two peaks have considerably different relative intensities than do those for the former two liquids. We shall return to this idea later, but for the moment, it is not immediately apparent, on the basis of the physical parameters of these liquids, why these peak intensities should be so different. As can be seen in Table 1, the quadrupole moments of HFB and TFB differ by an order of magnitude, so this does not seem to be a primary factor in determining the shape of the RSDs. The masses of TFB and HFB are significantly greater than that of benzene, and there is an even larger difference in the tumbling moments of inertia. It is thus possible, along the lines suggested by Ryu and Stratt,²⁶ that the frequencies of the modes that correspond to hindered rotations are shifted more than those due to hindered translations in going from benzene to HFB and TFB. With this in mind, it is interesting to note that, at any given temperature, the RSDs of HFB and TFB are quite similar without any frequency scaling being performed for their masses or moments of inertia, and in fact, such scaling lessens the similarity considerably. In addition,

Ryu and Stratt presented a scaling argument suggesting that translational modes should be most important when the isotropic polarizability is larger than the polarizability anisotropy.²⁶ However, whereas the isotropic polarizabilities of benzene, HFB, and TFB are virtually identical, the polarizability anisotropies of HFB and TFB are significantly larger than that of benzene. Thus, the scaling argument would predict that the translational contribution to the RSDs of HFB and TFB should be smaller than that for benzene.

An interesting contrast is provided by the RSDs for mesitylene. At high temperature, the mesitylene RSDs closely resemble those of HFB and TFB, albeit with a temperature shift on the order of 100 K. At low temperature, the mesitylene RSDs resemble those of benzene at low temperature, except that there is clearly an additional, sharp low-frequency feature in the mesitylene RSDs. Mesitylene thus seems able to span the range of shapes seen in the RSDs of all of the other liquids. The molecular weight and moment of inertia of mesitylene are similar to those of TFB. However, the ratio of the isotropic polarizability to the polarizability anisotropy of mesitylene is similar to that of benzene, as is the quadrupole moment. It is not immediately clear which, if any, of these parameters might play a role in causing mesitylene to go from having a benzene-like RSD at low temperature to having an HFB-like RSD at high temperature.

IV. Discussion

As discussed above, RSDs for simple liquids are often fit to the sum of a Bucaro–Litovitz function and an antisymmetrized Gaussian. These two spectral shapes are given by

$$g_{BL} = \omega^\delta \exp(-\omega/\omega_0) \quad (4)$$

and

$$g_{AG} = \exp[-(\omega - \omega_1)^2/2\sigma^2] - \exp[-(\omega + \omega_1)^2/2\sigma^2] \quad (5)$$

respectively. Although there is not a clearly assignable physical interpretation to such fits, it is still instructive to use this approach to compare the data for the different liquids studied here and to have a means of quantifying some of the temperature trends.

The fits to the BL line shape plus the AG line shape meet with varying degrees of success in the different liquids. The fits work quite well for benzene and benzene-*d*₆, as would be expected from previous work.^{19,31,38,41} On the other hand, it is clear from inspection of the mesitylene RSDs that any fit with only two modes will not be satisfactory. Both HFB and TFB are intermediate cases in which the fits are accurate at high frequencies but break down to some extent at low frequencies, as is illustrated for TFB at 335 K in Figure 9.

In Figure 10, we plot the parameters δ and ω_0 for the BL portion of the fits for benzene, benzene-*d*₆, HFB, and TFB. The same basic trends hold for all of the liquids for these two parameters. The exponent δ increases linearly with temperature. The slope of this increase is the same for benzene and benzene-*d*₆. The slopes for TFB and HFB are also the same, but are about 25% smaller than that for benzene. At any given temperature, the value of δ decreases roughly linearly with the inverse of the molecular weight, although the low-frequency portions of the fits to the data for TFB and HFB are poor enough that this might not be a meaningful correlation. The frequency ω_0 decreases with temperature. For benzene and benzene-*d*₆, this parameter appears to be decreasing toward a high-

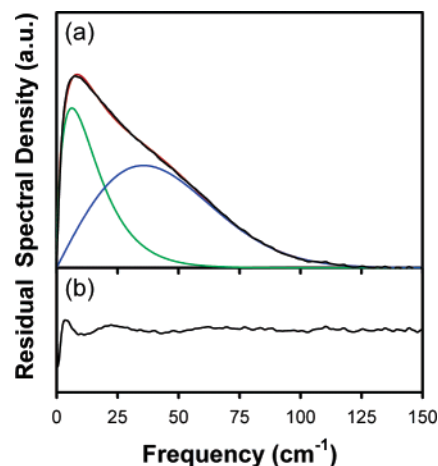


Figure 9. (a) RSD for TFB at 335 K (black), along with fit (red) to the sum of a Bucaro–Litovitz line shape (green) and an antisymmetrized Gaussian (blue). (b) Difference between the data and the fit.

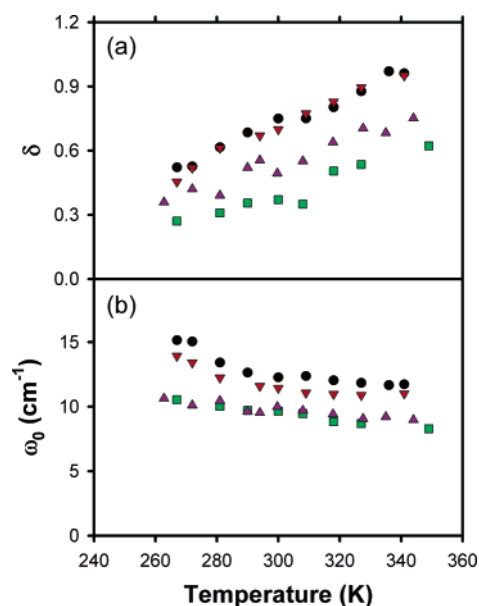


Figure 10. Parameters (a) δ and (b) ω_0 from the fits to the Bucaro–Litovitz line shape portion of the RSD for benzene (black), benzene-*d*₆ (red), HFB (green), and TFB (purple).

temperature asymptote, whereas for HFB and TFB, it decreases linearly. The value of ω_0 at any given temperature is smaller for benzene-*d*₆ than it is for benzene, and it is smaller still for HFB and TFB. However, the values for HFB and TFB are nearly identical to one another, so again, it is not clear whether there is any meaningful scaling with molecular weight. For benzene and benzene-*d*₆, however, the ratio of ω_0 values averaged over the temperatures at which we have data for both liquids is 1.09, which is close to the value of 1.1 that would be expected if this frequency were determined by the inverse square root of the moment of inertia.

The parameters ω_1 and σ for the AG portion of the fits for these liquids are shown in Figure 11. Here, as would be expected from the RSDs, there are dramatic differences between benzene and benzene-*d*₆ on one hand and HFB and TFB on the other. For benzene and benzene-*d*₆, the frequency ω_1 decreases with increasing temperature, as would be anticipated given that the intermolecular potential softens with decreasing density. The ratio between values of ω_1 at any given temperature is roughly 1.1, which would be expected if the frequency of this band scaled inversely with the square root of the moment of inertia.

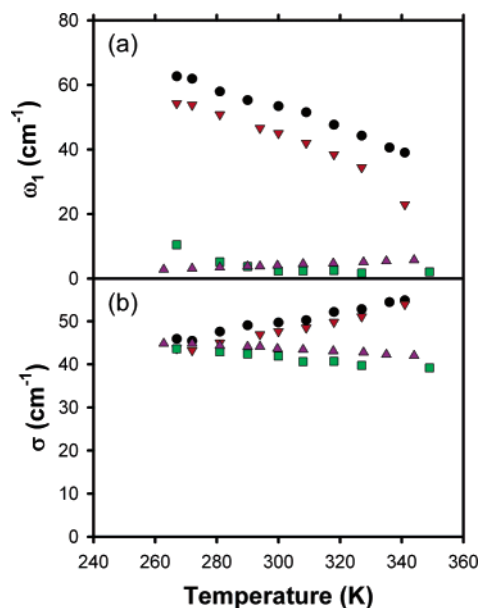


Figure 11. Parameters (a) ω_1 and (b) σ from the fits to the Gaussian line shape portion of the RSD for benzene (black), benzene- d_6 (red), HFB (green), and TFB (purple).

The values of ω_1 for HFB and TFB are an order of magnitude smaller than those for benzene and benzene- d_6 . Whereas the value of ω_1 for HFB decreases with temperature, as was the case for benzene and benzene- d_6 , the value for TFB increases with temperature. The behavior of σ is equally puzzling. For benzene and benzene- d_6 , σ increases with temperature and is roughly the same for the two liquids. This is the behavior that would be expected with a decreasing density. For HFB and TFB, however, σ is again roughly the same but decreases with increasing temperature.

We should again stress that great care should be taken in ascribing any direct physical meaning to the fit parameters for these liquids. The major significance of the differences among the AG fit parameters for these liquids might be merely the obvious, i.e., that the RSDs for HFB and TFB are qualitatively different from those of benzene and benzene- d_6 . Despite the fact that these fits work well at high frequencies for HFB and TFB, the AG function might not be an adequate descriptor of spectra that are so triangular. In looking at the TFB RSDs, for instance, it is easy to imagine that the high-frequency “peak” does increase in frequency with decreasing temperature. Indeed, the first moment of the TFB RSD does grow by about 10% in going from the highest temperature studied here to the lowest. The behavior of the first moment is opposite to that of ω_1 in the fits discussed above, but ω_1 is not directly indicative of the first moment of the AG function because of a strong interplay between this parameter and σ .

We now consider the RSD of mesitylene. As noted above, the RSD for this liquid has a low-frequency feature that becomes quite sharp at low temperatures, something that, to our knowledge, has not been reported for any other simple liquid. In considering the results for the time-domain fits presented in Figures 4 and 5, it is somewhat surprising that the RSDs for mesitylene at low temperature are so different from those of HFB and TFB. In all three liquids, the intermediate response time tracks the collective orientational correlation time, and a plot of τ_i versus τ_{or} falls on the same line. The normalized amplitudes of the intermediate response are approximately the same for all three liquids as well. The feature of mesitylene that makes it so special is that it has a large temperature range

over which it remains a liquid. The RSD of mesitylene at 434 K is similar to those of HFB and TFB at a temperature that is 100 K lower. The melting points of HFB and TFB are 277 and 268 K, respectively (the data presented here at the lowest temperatures for these two liquids are in the supercooled regime). We might then expect the RSD of mesitylene at approximately 370 K to resemble those of HFB and TFB near their melting points. The mesitylene RSD at 381 K does indeed resemble the RSDs of HFB and TFB at 267 K.

Approached from the opposite perspective, barring the sharp feature at low frequency, the RSDs of mesitylene at low temperatures strongly resemble those of benzene and benzene- d_6 at similar temperatures. The differences at low frequency are to be expected on the basis of the behavior of the intermediate response. This response has hydrodynamic behavior and tracks the collective orientational correlation time. Because the orientational correlation time of mesitylene is considerably longer than that of benzene at any given temperature, the mesitylene RSD would be expected to extend to lower frequencies than the benzene RSD.

It is worth considering whether the intermediate response is the major source of differences among the RSDs of simple liquids. The intermediate response time scales with the orientational correlation time as the temperature is varied for every simple, nonnetworked liquid we have studied.^{16,20} Given that this behavior has held for 20 different liquids, including those here, we can safely assume that it is an essentially universal feature within this class of liquids. As an empirical rule, we can thus say that the low-frequency portion of the RSD (i.e., the rising edge, which generally covers frequencies of $<20 \text{ cm}^{-1}$) is influenced by the collective orientational correlation time. The remainder of the RSD should similarly be related to the librational frequency of the molecules, which is determined in part by the moment of inertia of the molecules (although the intermolecular potential plays an equally important role). We can use this idea to explain the differences between the RSDs of benzene and CS_2 , for example. Benzene has a smaller moment of inertia than does CS_2 , but a longer collective orientational correlation time. We would therefore expect the benzene RSD to stretch farther to high and low frequency than does the CS_2 RSD at the same temperature, which is indeed what is observed.

Ratajska-Gadomska²¹ and, independently, Ryu and Stratt²⁶ made a similar suggestion previously, except that they attributed the low-frequency portion of the RSD to effects from hindered translational motions of molecules. The results presented here give us the opportunity to assess this idea experimentally. Although we cannot provide a definitive conclusion based on our data, a number of lines of evidence point to translations playing an insignificant role in OKE RSDs. First, as discussed above, the intermediate response clearly behaves hydrodynamically and is tied to the collective orientational correlation function in the same manner for a broad range of liquids. Orientational diffusion and density fluctuations are coupled, but it would be surprising if the coupling were this direct. Second, as also discussed above, a comparison of the RSDs for benzene and benzene- d_6 at the same temperature shows that scaling the frequencies by the inverse square root of the moment of inertia leads to nearly identical spectra. Third, Ryu and Stratt made a scaling argument²⁶ suggesting that, when the isotropic polarizability is larger than the polarizability anisotropy, hindered translations should play a greater role in the low-frequency RSD. According to this argument, HFB and TFB would be expected to have a less prominent low-frequency portion of the RSD than

benzene, but in fact, the opposite is the case. Finally, the simulations of Chelli et al. suggest that single-molecule (i.e., librational) scattering dominates the low-frequency Raman spectrum of benzene.³⁴ Taken together, these results strongly suggest that hindered orientations are primarily responsible for the shape of the RSD.

It is informative to consider why our results lead to a different conclusion than was reached from the simulations of Ryu and Stratt.²⁶ Whereas their simulations suggested that even for CS₂ there is a significant translational contribution to the RSD, our previous simulation work on CS₂ indicated that density fluctuations play virtually no role in depolarized light scattering for this liquid.⁶² The major difference between the two simulations is that Ryu and Stratt used a point anisotropic polarizability for each molecule,²⁶ whereas we used a distributed polarizability.⁶² Whereas point molecular polarizabilities would be expected to work well to describe light scattering in media that are not dense, their applicability in dense media such as liquids is questionable. The polarizability of a molecule is necessarily spread throughout the molecule, and it is important to take this into account when many-body effects, such as interaction-induced scattering, are being investigated. The fact that the use of a point anisotropic polarizability should overestimate the importance of translational effects in dense media is inherent in the scaling argument presented by Ryu and Stratt.²⁶ This argument was based on point molecular polarizabilities and, so, would be expected to apply to a simulation that uses such a model. In such a model, three-body effects, which lead to cancellations in interaction-induced scattering, are significant only when the centers of the three bodies are in close proximity. The larger the molecule being simulated, the less likely this is to be the case. However, in real liquids, three-body effects depend on the electron clouds of three molecules being in close proximity. This criterion is easily met and affects the translational contribution to depolarized scattering disproportionately because the translation of a single molecule does not change the principal axes of its polarizability tensor. Rotation of a molecule does affect the principal axes of this tensor, which tends to mitigate three-body effects.

To test whether the intermediate response is responsible for the major differences in RSDs among these liquids, we can remove this response from the time-domain data and calculate modified RSDs. Note that this subtraction does not necessarily yield a physically meaningful spectrum. For instance, if the intermediate response arises from motional narrowing of an otherwise broader low-frequency spectrum, it is not clear what interpretation should be given to the spectrum after this portion has been removed. Also, as is the case when removing the diffusive reorientation, there is no rigorous means of choosing a rise time, and subtracting two exponentials adds further uncertainty to the RSD. Nevertheless, computing such modified RSDs does give us the opportunity to make additional qualitative comparisons of the data.

In Figure 12, we plot the modified RSDs for benzene, benzene-*d*₆, and mesitylene, and in Figure 13, we plot the modified RSDs for HFB and TFB. A number of notable features are evident in comparing the modified RSDs. First, for all of the liquids, there are two clear spectral features at low temperature that merge into a single feature at high temperature. The modified RSDs of benzene and benzene-*d*₆ are strikingly similar to the RSDs of CS₂ and acetonitrile. The modified RSDs of HFB and TFB bear more similarity to those of benzene than did the unmodified RSDs, but the shapes for HFB and TFB are still quite distinct. The modified RSDs for mesitylene once again

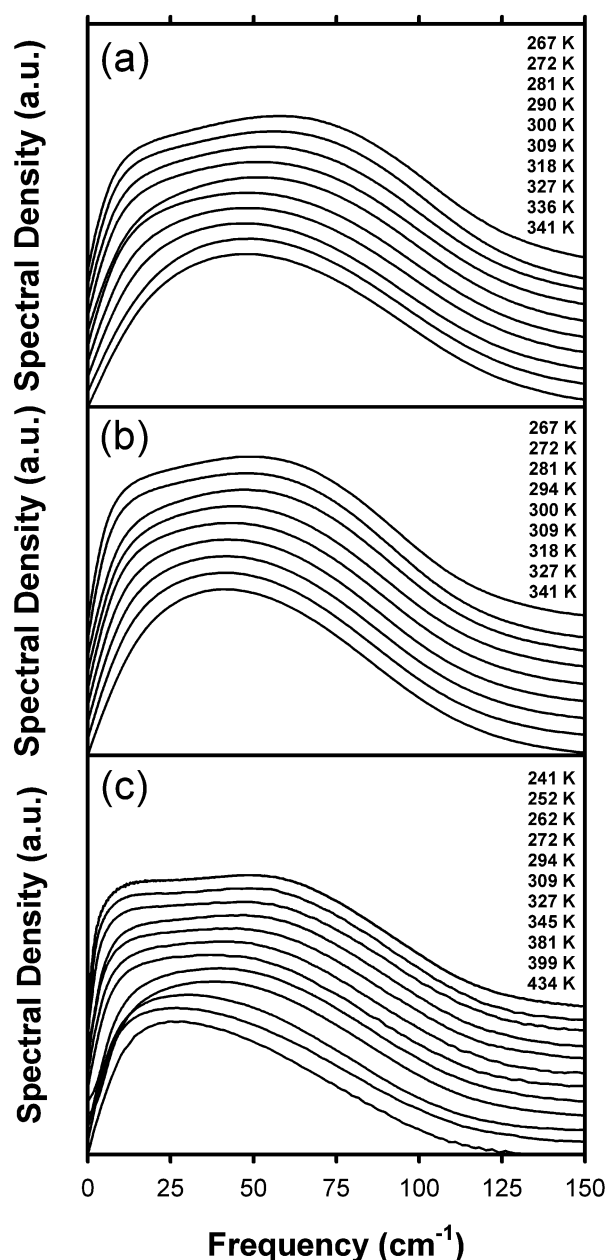


Figure 12. Modified RSDs for (a) benzene, (b) benzene-*d*₆, and (c) mesitylene. The heights of the RSD have been normalized, and the offsets are for clarity.

resemble those of benzene and benzene-*d*₆ at low temperature and those of HFB and TFB at high temperature. Finally, in all cases, there is still a low-frequency feature that moves to lower frequencies as the temperature is reduced, which further underscores the fact that the modified RSD is useful only for qualitative comparisons.

The sum of a BL function and an AG function does an excellent job of fitting the modified RSDs for all of the liquids. Shown in Figure 14 is a fit to the modified RSD of TFB at 335 K. The residual is quite flat and is typical of the fits for all of the liquids. The parameters for these fits are plotted in Figures 15 and 16 as a function of temperature. Although the data are noisier, the same basic trends appear to hold for the BL fit as did in the case of the unmodified RSDs, except that the frequency ω_0 now increases to some extent with increasing temperature. The ω_1 parameter for the AG portion of the fit to the modified RSDs no longer differs so substantially for HFB and TFB versus benzene and benzene-*d*₆. However, ω_1 does

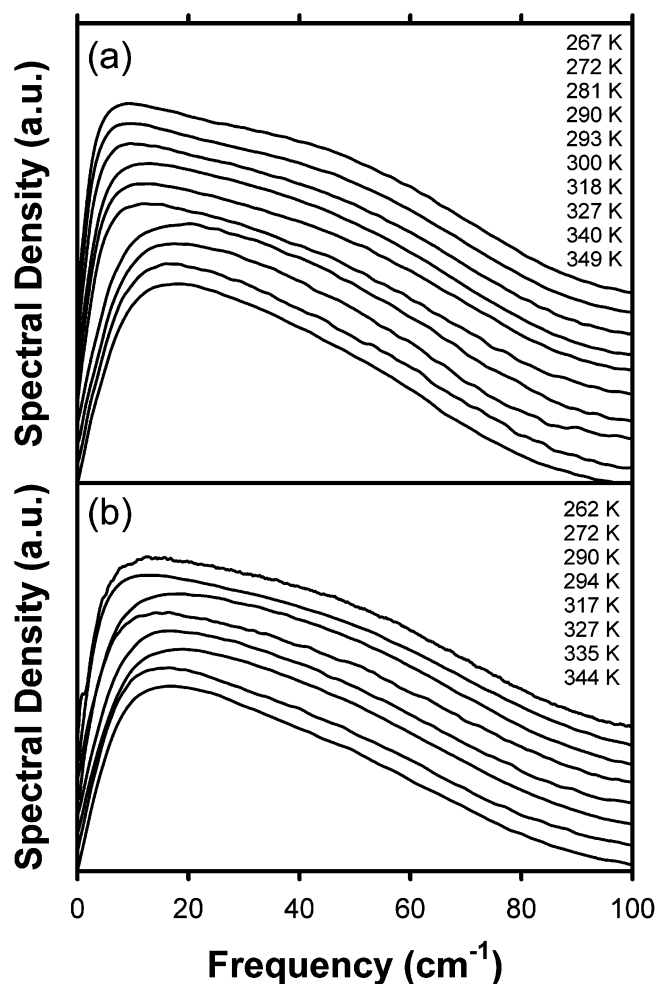


Figure 13. Modified RSDs for (a) HFB and (b) TFB. The heights of the RSDs have been normalized, and the offsets are for clarity.

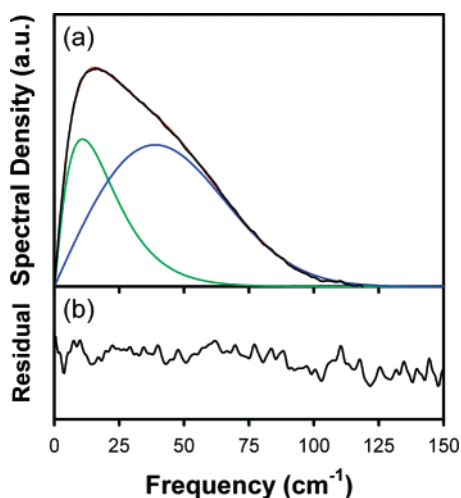


Figure 14. (a) RSD for TFB at 335 K (black) corresponding to the OKE decay with two exponentials subtracted, along with fit (red) to the sum of a Bucaro–Litovitz line shape (green) and an antisymmetrized Gaussian (blue). (b) Difference between the data and the fit.

increase with temperature for HFB and TFB, whereas for the other three liquids, it decreases. In addition, the width σ decreases with temperature for HFB and TFB, whereas the other three liquids exhibit a more intuitive increased broadening with increasing temperature.

The most important qualitative conclusion that we can draw from these modified RSDs is that, whereas, empirically, the

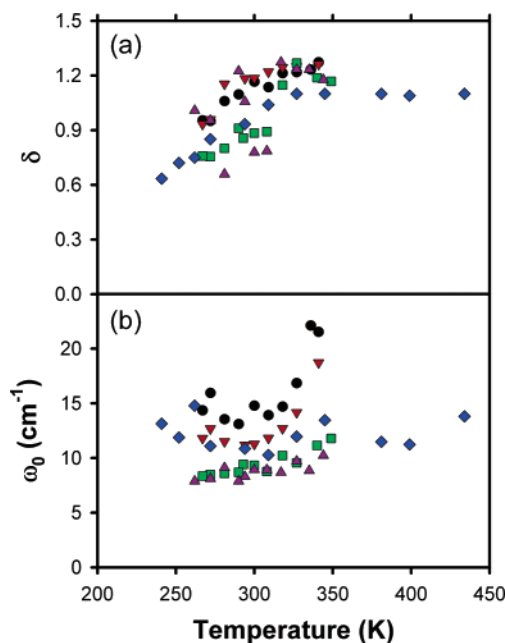


Figure 15. Parameters (a) δ and (b) ω_0 from the fits to the Bucaro–Litovitz line shape portion of the RSD corresponding to the OKE decay with two exponentials subtracted for benzene (black), benzene- d_6 (red), HFB (green), TFB (purple), and mesitylene (blue).

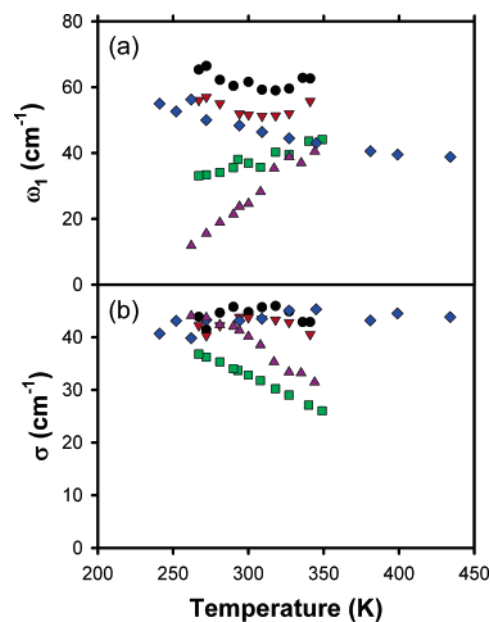


Figure 16. Parameters (a) ω_1 and (b) σ from the fits to the Gaussian line shape portion of the RSD corresponding to the OKE decay with two exponentials subtracted for benzene (black), benzene- d_6 (red), HFB (green), TFB (purple), and mesitylene (blue).

intermediate response might determine the behavior of the low-frequency portion of the RSD, the shape of the remainder of the RSD is not determined solely by anything as simple as scaling with the square root of the moment of inertia of the molecule. We must therefore search for other clues as to the differences among the RSDs of these liquids.

One factor that the data presented here allow us to discount in determining the differences in the shapes of the RSDs of the liquids studied here, to a large extent, is molecular shape. All of the molecules studied here are disklike, but the RSDs for HFB and TFB differ considerably from those of benzene and benzene- d_6 . The size and shape of mesitylene are quite similar to those of TFB, and yet mesitylene's RSDs are more similar

to those of benzene than to those of TFB. Furthermore, if we take into account the idea that the low-frequency feature is linked directly to the orientational correlation time, the RSDs of benzene, benzene- d_6 , and mesitylene are quite similar to those of linear molecules such as CS_2 and acetonitrile. Viewed in this light, the real task here might be to explain why the RSDs of HFB and TFB are so different from those of any other liquid.

There are two basic microscopic mechanisms for generating the depolarized light scattering that is the basis of the OKE signal.^{63,64} Molecular depolarized scattering arises from changes in the orientations of individual molecules that have anisotropic polarizabilities. Interaction-induced (I-I) scattering arises from interactions among polarizable molecules, and at the simplest level, it can be described in terms of dipole-induced dipole interactions. I-I scattering is necessarily a many-body effect and can be observed even if there is no molecular polarizability anisotropy, such as in fluids composed of atoms or highly symmetric molecules.^{65–67} Both orientational and translational motions can contribute to I-I scattering.⁶² As discussed above, we feel that there are strong grounds to believe that, in liquids composed of molecules with anisotropic polarizabilities, orientational effects are the major contributor to depolarized I-I scattering.⁶²

Because the OKE signal depends on the correlation of the collective polarizability at two different times, there is a cross term between molecular and I-I scattering. This cross term is generally negative, whereas fits to OKE RSDs generally involve functions that are all positive. It is therefore possible that the differences among the spectra for the different liquids presented here arise from differing degrees of cancellation. However, the cross term generally takes on a shape that is similar to that of the molecular component of the scattering, and so, the sum of these two components also has a similar shape.⁶⁸ It is therefore reasonable to fit OKE RSDs solely to positive functions, and it is unlikely that this cross term has a strong effect on the shape of the RSDs.

Although the shapes of the molecules studied here are all disklike, the electronic distributions of the molecules differ considerably. Single parameters such as the isotropic polarizability or the polarizability anisotropy offer little insight into what portion of a molecule is most readily polarized. Both mesitylene, with its electron-donating methyl groups, and benzene would be expected to be most polarizable in the π -electron clouds. On the other hand, as would be suggested by its opposite quadrupole moment, HFB would be expected to be most polarizable at its strongly electron-withdrawing fluorine atoms. Furthermore, the π electrons of benzene are highly delocalized, whereas the electrons on the fluorine atoms in HFB are not. If this effect were responsible for the differences in the benzene and HFB RSDs, then the behavior of the TFB RSDs would be expected to be somewhere between those of the other two liquids, which is not the case. Furthermore, the distribution of the polarizability cannot explain why the mesitylene RSDs are benzene-like at low temperature but resemble those of HFB and TFB at high temperature.

Another possible explanation for the differences in the spectra is that there are differences in local liquid structure. This would be a desirable explanation, in that it would suggest that OKE spectra can provide qualitative microscopic structural information. Fortunately, detailed information is available on the microscopic structures of benzene, HFB, and TFB, allowing us to assess the role that this structure might play in determining the shape of the RSD.

Judging from the similar shapes of benzene, HFB, and TFB, it might be imagined that the local structures are similar in all of these liquids. This is not the case, however. Cabaço and co-workers^{43,45,48–51} and others⁶⁹ performed a series of neutron-scattering experiments and molecular dynamics simulations on these three liquids and found significant local structural differences among them. In the crystalline form of benzene, the molecules arrange themselves in a herringbone pattern.⁷⁰ This observation led to the suggestion, which was later supported by both theory⁷¹ and X-ray scattering data,⁷² that perpendicular structures are favored in liquid benzene as well. Cabaço and co-workers found that all angles between benzene nearest neighbors are almost equally likely, although there is a slight preference for the molecules to either be parallel (but offset) or perpendicular.^{43,45} This result is in good agreement with the observed value of approximately unity for $g_{2/2}$ in this liquid.⁷³

Presumably, the nuances of the local structure of benzene derive from the relatively large quadrupole moment of this molecule, which can lead to repulsive interactions that change the effective shape of the molecule. The quadrupole moment of HFB is nearly equal in magnitude to that of benzene, but opposite in sign. On this basis, HFB might be expected to have a local structure that is similar to that of benzene, but in fact, this is not the case. HFB shows a relatively strong preference for adopting a parallel but offset structure of nearest-neighbor molecules with all other angles between nearest neighbors being relatively equally likely,^{43,51} which is again in good agreement with the observed value of $g_{2/2}$. These differences might be due in part to the different aspect ratios of benzene and HFB. In addition, at liquid densities, the quadrupole moment cannot provide an adequate description of the electrostatic interactions that contribute to local structure. It is the charge distribution of the molecules that is important in short-range interactions, and a given quadrupole moment is consistent with many such charge distributions.

The local structure of TFB differs considerably from those of both benzene and HFB. As discussed above, TFB has a strong tendency to form face-to-face dimers in the liquid. All other local structures are roughly equally likely but are far less prevalent than the face-to-face structure,^{43,48,50} which is consistent with the large value of ρ for this liquid. The relatively small quadrupole moment of this molecule leads to a considerably smaller repulsion in the face-to-face geometry, which is probably further overcome by favorable octupole–octupole interactions for dimers in which the two molecules are rotated by 60° relative to each other.

On the basis of what is known about the local structures of benzene, HFB, and TFB, we can propose a model that can explain the differences among the RSDs of these liquids. We begin by assuming that the librational frequencies of the liquid molecules depend to some extent on whether individual molecules participate in parallel versus perpendicular structures. There is some support for this conjecture in the INM work of Ryu and Stratt, who found that the contribution to the INM density of states from hindered tumbling motions is bimodal,²⁶ although they did not address how the frequency of this motion correlated to local structure. Benzene is the liquid with the greatest degree of perpendicular ordering among those considered here, and it also has the greatest intensity in the high-frequency region of the RSD. We therefore further assume that perpendicular structures have higher librational frequencies than do structures in which molecules are parallel. Because benzene has roughly equivalent numbers of molecules in parallel and perpendicular local structures, it might be expected to have two

features in the RSD that are roughly of equal intensity. As the temperature is increased, the proportion of perpendicular local structures is relatively constant, so we can view the spectral changes as resulting largely from changes in the density and the intermediate relaxation.

At the opposite extreme, the RSD of TFB would be expected to be dominated by a low-frequency feature from parallel molecules, with a weaker feature due to perpendicular molecules. The fraction of perpendicular molecules in this liquid increases modestly with increasing temperature, as evidenced from simulations^{49,50} and the value of g_2/j_2 . The increase of the ω_1 parameter of the AG portion of the fits to the TFB RSDs with increasing temperature might be a reflection of this modest increase in population of structures with higher librational frequencies, which could counteract the decrease in density with temperature.

The behavior of HFB would be expected to be intermediate between those of benzene and TFB. HFB exhibits a high degree of parallel ordering, but there are significant numbers of molecules in perpendicular and other orientations as well.⁵¹ We would therefore expect the RSD of this liquid to be dominated by the lower-frequency feature, but with a more prominent higher-frequency feature than for TFB. Judging from the values of g_2/j_2 and from simulations,⁵¹ the relative populations of different local orientational states in HFB change modestly with temperature, with perpendicular structures becoming somewhat more favored. The increase in intensity at high frequencies that would be expected from this change in structure might be compensated by density changes.

We next turn to the case of mesitylene. Although no temperature-dependent scattering data or simulations are available for this liquid, we can make some predictions about the local structure and its temperature dependence on the basis of g_2/j_2 . As shown in Figure 3, the behavior of this ratio is somewhat unusual, in that it grows larger with increasing temperature, implying that the degree of parallel ordering increases as well. An increase in parallel ordering with increasing temperature is completely in line with the RSDs of mesitylene, which go from resembling those of benzene at low temperature to resembling those of HFB and TFB at high temperature.

Is it reasonable to believe that perpendicular configurations of disklike molecules should, on average, have higher librational frequencies than parallel configurations? To answer this question, it is important to consider not isolated pairs of molecules, but rather pairs of molecules within a closely packed liquid. The crystal structure of benzene is a herringbone pattern in which the local structure is roughly perpendicular,⁷⁰ which suggests that this is the form in which the molecules can pack most tightly and therefore would be most likely to have higher librational frequencies. This idea is further supported by the work of Lowden and Chandler,⁷¹ who demonstrated that a hard-core model of benzene is consistent with a liquid with considerable perpendicular structure. HFB also crystallizes in a herringbone structure,⁷⁴ which suggests that the relatively high degree of parallel ordering found in the liquid results in comparatively inefficient packing and therefore lower librational frequencies. The density of HFB increases considerably more ($\sim 22\%$)⁷⁵ than does that of benzene ($\sim 17\%$) upon crystallization, which further supports this idea. Presumably, the same argument should hold for TFB, although its crystal structure features parallel stacks of molecules with alternating orientations.⁷⁶ However, this efficient parallel packing of TFB is due to its ability to form face-to-face parallel structures, which are energetically unfavorable in the other liquids. In liquid TFB,

the parallel structures are not just face-to-face, but rather cover a broad range of relative positions.^{49,50} In addition, the density increase of TFB upon crystallization is comparable to that of HFB.⁷⁶ We therefore might still expect parallel structures in liquid TFB to have lower average librational frequencies than perpendicular local structures.

As another test of these ideas, we can compare the OKE spectra of these liquids to low-frequency Raman data from the corresponding crystals. Such data are available for benzene,⁷⁷ HFB,⁷⁸ and TFB.⁷⁹ As discussed above, both benzene⁷⁰ and HFB⁷⁴ crystallize in a herringbone pattern, although the crystal structures are somewhat different for the two substances. Whereas the low-frequency Raman spectrum of crystalline benzene⁷⁷ bears strong resemblance to its OKE spectrum in the liquid,^{21,35} the same cannot be said for the low-frequency Raman spectrum of crystalline HFB.⁷⁸ This result is in good agreement with the relatively large degree of parallel ordering in liquid HFB,⁵¹ which differs considerably from the case in the crystal. In the case of TFB, the OKE spectrum in the liquid is highly reminiscent of the low-frequency Raman spectrum in the crystalline state,⁷⁹ which is consistent with the high degree of parallel ordering in both phases.

It is worthwhile to compare our model to the models of Chelli et al.³⁴ and Ratajska-Gadomska.²¹ Chelli et al. proposed, on the basis of simulations and experimental data, that the low-frequency portion of the intermolecular Raman spectrum could be interpreted in terms of transient shells of nearest-neighbor molecules about a central molecule.³⁴ The intermediate response could then be related to the rearrangement of these local cages.³⁴ Ratajska-Gadomska adopted a related approach in which the local cages were assumed to have structures related to that of crystalline benzene.²¹ Although our model approaches the structure of the RSD from a different viewpoint, it is not inconsistent with these other models. It might well be, for instance, that local cages that have a large degree of parallel ordering tend to promote lower librational frequencies for the central molecule. This idea is worth further investigation.

We should also consider whether the local structure model might provide insights into the OKE spectra of liquids that are not composed of disklike molecules. The other liquids for which the most detailed temperature-dependent information is available are CS₂ and acetonitrile.¹⁵ Both of these molecules are linear and, so, would be expected to have a considerable degree of parallel local structure in the liquid phase. As discussed above, for both liquids, the RSD is a smooth function at high temperature, but as the temperature is lowered, the high-frequency portion moves to higher frequencies and the low-frequency portion to lower frequencies. The change in the spectra is striking, especially for CS₂ with its large liquid temperature range. In analogy, for the model for disklike molecules, we can posit that, in the case of linear molecules, it is parallel local structures that have the highest librational frequencies. As the temperature is increased, g_2/j_2 is known to decrease for both acetonitrile and CS₂.¹⁶ This indicates a decrease in local parallel structure that works in concert with a decrease in density to move the high-frequency portion of the spectrum to lower frequencies. Furthermore, g_2/j_2 for acetonitrile is significantly larger than the value for CS₂,¹⁶ which would suggest that the former liquid should have a more prominent high-frequency feature in its RSDs. This prediction is borne out by experiment.¹⁵

V. Conclusions

We have presented a detailed, temperature-dependent OKE study of five aromatic liquids. Despite the disklike shape of all

of the molecules, the behavior of the HFB and TFB OKE spectra is qualitatively different from that of benzene and benzene- d_6 , with mesitylene lying somewhere in between. Comparison of the RSDs for the different liquids allows us to make a case that translational motions are relatively unimportant in the spectra. Our data support the idea that the OKE RSD reflects the distribution of local structures in these liquids. Although we have couched our model in terms of parallel versus perpendicular local structures, these are of course only extremes in a continuum of possible local structures. Although it might not be possible to extract all of the features of this continuum directly from OKE spectra, if correct, our model still offers the possibility of being able to draw a specific, qualitative connection between the shape of the OKE spectrum of a liquid and its microscopic properties.

The basic picture that we propose to explain the shape of the OKE spectrum is as follows: The intermediate response determines the appearance of the low-frequency edge of the OKE RSDs through hydrodynamic effects. The shape of the remainder of the spectrum is influenced by the local structuring of the liquid and by the shape of the molecules, insofar as the shape determines which local structures will have lower or higher librational frequencies. The overall frequency range that the OKE spectrum covers is also influenced by the density, which has a direct effect on the librational potential. One important implication of this model is that g_2 might be a good predictor of the shape of the OKE spectrum once molecular shape is taken into account.

All of the expectations of our simple local structure model are borne out by the experimental data, but further testing of this idea is required. Such testing will include experiments on other liquids, but these ideas need to be tested with MD simulations as well, which is being done currently by another group.⁸⁰ It would be interesting, for instance, to explore whether the INM frequencies observed for tumbling librations in benzene correlate with local structure. It would also be useful to perform similar analyses on the other liquids studied here. Furthermore, if this model is correct, our data suggest that mesitylene should have a higher degree of perpendicular local structure at low temperature and that the degree of parallel structuring should increase with temperature. Temperature-dependent neutron scattering experiments or MD simulations for this liquid could provide a crucial test of this model.

Acknowledgment. We are grateful to Prof. Paul Madden for providing us with Raman data for HFB, TFB, and mesitylene. We are also grateful to Prof. Hiroko Shimada for providing us with ref 78. This work was supported by the National Science Foundation, Grants CHE-0314020 and CHE-0073228. J.T.F. is a Research Corporation Cottrell Scholar and a Camille Dreyfus Teacher-Scholar.

Supporting Information Available: Fit parameters for the integrated OKE decays and reduced spectral densities for each liquid studied here. This material is available free of charge via the Internet at <http://pubs.acs.org>.

References and Notes

- Fourkas, J. T. In *Ultrafast Infrared and Raman Spectroscopy*; Fayer, M. D., Ed.; Marcel Dekker: New York, 2001; Vol. 26, p 473.
- Righini, R. *Science* **1993**, 262, 1386.
- Kinoshita, S.; Kai, Y.; Ariyoshi, T.; Shimada, Y. *Int. J. Mod. Phys. B* **1996**, 10, 1229.
- Smith, N. A.; Meech, S. R. *Int. Rev. Phys. Chem.* **2002**, 21, 75.
- McMorrow, D.; Lotshaw, W. T. *Chem. Phys. Lett.* **1990**, 174, 85.
- McMorrow, D. *Opt. Commun.* **1991**, 86, 236.
- McMorrow, D.; Lotshaw, W. T. *J. Phys. Chem.* **1991**, 95, 10395.
- Berne, B. J.; Pecora, R. *Dynamic Light Scattering*; Wiley: New York, 1976.
- Kalpouzos, C.; Lotshaw, W. T.; McMorrow, D.; Kenney-Wallace, G. A. *J. Phys. Chem.* **1987**, 91, 2028.
- Lotshaw, W. T.; McMorrow, D.; Kalpouzos, C.; Kenney-Wallace, G. A. *Chem. Phys. Lett.* **1987**, 136, 323.
- Deeg, F. W.; Fayer, M. D. *J. Chem. Phys.* **1989**, 91, 2269.
- McMorrow, D.; Lotshaw, W. T. *Chem. Phys. Lett.* **1991**, 178, 69.
- Chang, Y. J.; Castner, E. W., Jr. *J. Chem. Phys.* **1993**, 99, 113.
- Neelakandan, M.; Pant, D.; Quitevis, E. L. *J. Phys. Chem. A* **1997**, 101, 2936.
- Farrer, R. A.; Loughnane, B. J.; Deschenes, L. A.; Fourkas, J. T. *J. Chem. Phys.* **1997**, 106, 6901.
- Loughnane, B. J.; Scodinu, A.; Farrer, R. A.; Fourkas, J. T.; Mohanty, U. *J. Chem. Phys.* **1999**, 111, 2686.
- Foggi, P.; Bartolini, P.; Bellini, M.; Giorgini, M. G.; Morresi, A.; Sassi, P.; Cataliotti, R. S. *Eur. Phys. J. D* **2002**, 21, 143.
- Smith, N. A.; Meech, S. R. *J. Phys. Chem. A* **2000**, 104, 4223.
- Ricci, M.; Bartolini, P.; Chelli, R.; Cardini, G.; Califano, S.; Righini, R. *Phys. Chem. Chem. Phys.* **2001**, 3, 2795.
- Zhu, X.; Farrer, R. A.; Zhong, Q.; Fourkas, J. T. *J. Phys. Condens. Matter* **2005**, 17, S4105.
- Ratajska-Gadomska, B. *J. Chem. Phys.* **2002**, 116, 4563.
- Chang, Y. J.; Castner, E. W., Jr. *J. Chem. Phys.* **1993**, 99, 7289.
- Chang, Y. J.; Castner, E. W., Jr. *J. Phys. Chem.* **1994**, 98, 9712.
- Neelakandan, M.; Pant, D.; Quitevis, E. L. *Chem. Phys. Lett.* **1997**, 265, 283.
- Bucaro, J. A.; Litovitz, T. A. *J. Chem. Phys.* **1971**, 54, 3846.
- Ryu, S.; Stratt, R. M. *J. Phys. Chem. B* **2004**, 108, 6782.
- Friedman, J. S.; She, C. Y. *J. Chem. Phys.* **1993**, 99, 4960.
- Kinoshita, S.; Kai, Y.; Yamaguchi, M.; Yagi, T. *Phys. Rev. Lett.* **1995**, 75, 148.
- Cong, P.; Simon, J. D.; She, C. Y. *J. Chem. Phys.* **1996**, 104, 962.
- Friedman, J. S.; Lee, M. C.; She, C. Y. *Chem. Phys. Lett.* **1991**, 186, 161.
- McMorrow, D.; Lotshaw, W. T. *Chem. Phys. Lett.* **1993**, 201, 369.
- Cong, P.; Deuel, H. P.; Simon, J. D. *Chem. Phys. Lett.* **1995**, 240, 72.
- Vohringer, P.; Scherer, N. F. *J. Phys. Chem.* **1995**, 99, 2684.
- Chelli, R.; Cardini, G.; Ricci, M.; Bartolini, P.; Righini, R.; Califano, S. *Phys. Chem. Chem. Phys.* **2001**, 3, 2803.
- Ratajska-Gadomska, B.; Gadomski, W.; Wiewior, P.; Radzewicz, C. *J. Chem. Phys.* **1998**, 108, 8489.
- Smith, N. A.; Lin, S.; Meech, S. R.; Yoshihara, K. *J. Phys. Chem. A* **1997**, 101, 3641.
- Smith, N. A.; Lin, S.; Meech, S. R.; Shiota, H.; Yoshihara, K. *J. Phys. Chem. A* **1997**, 101, 9578.
- Chang, Y. J.; Castner, E. W., Jr. *J. Phys. Chem.* **1996**, 100, 3330.
- Bartolini, P.; Ricci, M.; Torre, R.; Righini, R.; Santa, I. *J. Chem. Phys.* **1999**, 110, 8653.
- Shiota, H. *J. Chem. Phys.* **2005**, 122.
- Beard, M. C.; Lotshaw, W. T.; Kortner, T. M.; Heilweil, E. J.; McMorrow, D. *J. Phys. Chem. A* **2004**, 108, 9348.
- Ronne, C.; Jensby, K.; Loughnane, B. J.; Fourkas, J.; Nielsen, O. F.; Keiding, S. R. *J. Chem. Phys.* **2000**, 113, 3749.
- Cabaco, M. I.; Danten, Y.; Besnard, M.; Guissani, Y.; Guillot, B. *J. Phys. Chem. B* **1997**, 101, 6977.
- Cabaco, M. I.; Danten, Y.; Besnard, M.; Guissani, Y.; Guillot, B. *J. Phys. Chem. B* **1998**, 102, 10712.
- Tassaing, T.; Cabaco, M. I.; Danten, Y.; Besnard, M. *J. Chem. Phys.* **2000**, 113, 3757.
- Elola, M. D.; Ladanyi, B. M. *J. Chem. Phys.* **2005**, 122.
- Elola, M. D.; Landanyi, B. M.; Scodinu, A.; Loughnane, B. J.; Fourkas, J. T. *J. Phys. Chem. B* **2005**, 109, 24085.
- Cabaco, M. I.; Danten, Y.; Besnard, M.; Guissani, Y.; Guillot, B. *Chem. Phys. Lett.* **1996**, 262, 120.
- Cabaco, M. I.; Tassaing, T.; Danten, Y.; Besnard, M. *J. Phys. Chem. A* **2000**, 104, 10986.
- Cabaco, M. I.; Tassaing, T.; Danten, Y.; Besnard, M. *Chem. Phys. Lett.* **2000**, 325, 163.
- Danten, Y.; Cabaco, M. I.; Tassaing, T.; Besnard, M. *J. Chem. Phys.* **2001**, 115, 4239.
- Patterson, G. D.; Griffiths, J. E. *J. Chem. Phys.* **1975**, 63, 2406.
- Madden, P. A. Edinburgh University. Unpublished results, 2005.
- Debye, P. *Polar Molecules*; Dover: New York, 1929.
- Kivelson, D.; Madden, P. A. *Annu. Rev. Phys. Chem.* **1980**, 31, 523.
- Loughnane, B. J.; Farrer, R. A.; Scodinu, A.; Reilly, T.; Fourkas, J. T. *J. Phys. Chem. B* **2000**, 104, 5421.
- Dhar, L.; Rogers, J. A.; Nelson, K. A. *Chem. Rev.* **1994**, 94, 157.
- Scodinu, A.; Fourkas, J. T. *J. Phys. Chem. B* **2002**, 106, 10292.

- (59) Zhu, X.; Farrer, R. A.; Fourkas, J. T. *J. Phys. Chem. B* **2005**, *109*, 12724.
- (60) *SigmaPlot*, version 9.0; Systat: Point Richmond, CA, 2004.
- (61) *Chem 3D Pro*, version 5.0; CambridgeSoft: Cambridge, MA, 1999.
- (62) Murry, R. L.; Fourkas, J. T.; Li, W.-X.; Keyes, T. *Phys. Rev. Lett.* **1999**, *83*, 3550.
- (63) Keyes, T.; Kivelson, D.; McTague, J. P. *J. Chem. Phys.* **1971**, *55*, 4096.
- (64) Geiger, L. C.; Ladanyi, B. M. *J. Chem. Phys.* **1987**, *87*, 191.
- (65) Fleury, P. A.; Worlock, J. M.; Carter, H. L. *Phys. Rev. Lett.* **1973**, *30*, 591.
- (66) Greene, B. I.; Fleury, P. A.; Carter, H. L.; Farrow, R. C. *Phys. Rev. A* **1984**, *29*, 271.
- (67) Teboul, V.; Le Duff, Y. *J. Chem. Phys.* **1997**, *107*, 10415.
- (68) Keyes, T.; Kivelson, D. *J. Chem. Phys.* **1972**, *56*, 1057.
- (69) Steinhäuser, O.; Hausleithner, I. *Ber. Bunsen.-Ges. Phys. Chem.* **1988**, *92*, 781.
- (70) Jeffrey, G. A.; Ruble, J. R.; McMullan, R. K.; Pople, J. A. *Proc. R. Soc. (London) Ser. A* **1987**, *414*, 47.
- (71) Lowden, L. J.; Chandler, D. **1974**, *61*, 5228.
- (72) Narten, A. H. *J. Chem. Phys.* **1977**, *67*, 2102.
- (73) Madden, P. A.; Battaglia, M. R.; Cox, T. I.; Pierens, R. K.; Champion, J. *Chem. Phys. Lett.* **1980**, *76*, 604.
- (74) Boden, N.; Davis, P. P.; Stam, C. H.; Wesselink, G. A. *Mol. Phys.* **1973**, *25*, 81.
- (75) Bertolucci, M. D.; Marsh, R. E. *J. Appl. Crystallogr.* **1974**, *7*, 87.
- (76) Thalladi, V. R.; Weiss, H. C.; Blaser, D.; Boese, R.; Nangia, A.; Desiraju, G. R. *J. Am. Chem. Soc.* **1998**, *120*, 8702.
- (77) Bonadeo, H.; Marzocchi, M. P.; Castellucci, E.; Califano, S. *J. Chem. Phys.* **1972**, *57*, 4299.
- (78) Suzuki, Y.; Shimada, H.; Shimada, R. *Bull. Chem. Soc. Jpn.* **1996**, *69*, 3081.
- (79) Sakaki, N.; Ohno, Y.; Okabe, C.; Nibu, Y.; Shimada, H. *Fukuoka Daigaku Rigaku Shuho* **2002**, *32*, 29.
- (80) Elola, M. D.; Ladanyi, B. M. Colorado State University. Unpublished results, 2006.
- (81) Ruthven, D. M.; Kaul, B. K. *Ind. Eng. Chem. Res.* **1993**, *32*, 2053.
- (82) Debuschewitz, C.; Kohler, W. *Phys. Rev. Lett.* **2001**, *87*, 055901.
- (83) Wahid, H. *J. Opt.* **1995**, *26*, 109.
- (84) Hernandez-Trujillo, J.; Costas, M.; Vela, A. *J. Chem. Soc., Faraday Trans.* **1993**, *89*, 2441.